

316L

가

## Evaluation of residual stresses for the multipass welds of 316L stainless steel pipe

150

가가

. 316L

316L

ANSYS

(t/d=0.034)

18

(t/d=0.075)

가

### Abstract

It is necessary to evaluate the influence of the residual stress and distortion in the design and fabrication of welded structure and the sound welded structure can be maintained by this consideration. Multipass welds of the 316L stainless steel have been widely employed in the pipes of Liquid Metal Reactor. In this study, the residual stresses in the 316L stainless steel pipe welds were calculated by the finite element method using ANSYS code. Also, the residual stresses both on the surface and in the interior of the thickness were measured by HRPD(High Resolution Powder Diffractometer) instrumented in HANARO Reactor. The residual stresses were measured for each 18 points in small(t/d=0.075) and large pipe specimens (t/d=0.034). The experimental and calculated results were compared and the characteristics of the distribution of the residual stress discussed.

1.

. 가

(1).

가

가

가가

, , x

cm

(HRPD)

2.

Fig. 1

2

18

SMAW

350

mm/min

Table 1

316L

AWS A5.4

E316L-16

3

2

가

가

가

1.95 W/m<sup>2</sup>°C

1/2

(2).

Fig. 2

x

가

y

3.

HRPD

3가

calibration

d<sub>0</sub>

sample

stage

d

Ni-powder

Fig. 3  
Fig. 4

sample stage

X-Y

(Normal, Transverse, Longitudinal

(3).

4.

4.1

(1)

$$\frac{\partial}{\partial X_i} \left( k \frac{\partial T}{\partial X_i} \right) + Q = \rho c \frac{\partial T}{\partial t} \quad (1)$$

$$T(X_i, t=t_o) = T_o(X_i) \quad (2)$$

가 (3),(4),(5)

$$T(X_i, t) = \bar{T}(X_i, t) \quad (3)$$

$$-k_i \frac{\partial T}{\partial X_i} n_i = q \quad (4)$$

$$-k_i \frac{\partial T}{\partial X_i} n_i = h(T - T_e) \quad (5)$$

$n_i$  (component)  $h$  ,  $T_e$

(6)

$$-k_i \frac{\partial T}{\partial X_i} n_i = \sigma \varepsilon f(T^4 - T_e^4) \quad (6)$$

$\sigma$  (Stefan-Boltzman)  $\varepsilon$  ,  $f$

(2)

가 , 가 (5).

$$\varepsilon_{ij} = \varepsilon_{ij}^e + \varepsilon_{ij}^p + \varepsilon_{ij}^{th} \quad (7)$$

$$\varepsilon_{ij}^e = \frac{1+\nu}{E} \sigma_{ij} - \frac{\nu}{E} \sigma_{kk} \delta_{ij} \quad (8)$$

$\delta_{ij}$  : Kronecker symbol

$\nu$  :

$E$  :

$$\varepsilon_{ij}^p = \int_0^t \dot{\varepsilon}_{ij}^p dt \quad (9)$$

$$\varepsilon_{ij}^{th} = \alpha (T - T_o) \quad (10)$$

$\alpha$  ,  $T_o$  .  
 $t + \Delta t$

$${}^t \varepsilon_{ij} = {}^t \varepsilon_{ij}^e + {}^t \varepsilon_{ij}^p + {}^t \varepsilon_{ij}^{th} + {}^t \varepsilon_{ij}^{e'} \quad (11)$$

$${}^t \varepsilon_{ij}^p = \Delta t \Lambda^{t+\Delta t} \tau' \quad (12)$$

$${}^t \varepsilon_{ij}^{th} = {}^{t+\Delta t} \alpha {}^{t+\Delta t} T - {}^t \alpha {}^t T \quad (13)$$

$${}^t \varepsilon_{ij}^{e'} = \frac{\partial [C^E]^{-1}}{\partial T} \bullet \{ {}^t \tau \} dT \quad (14)$$

${}^t \varepsilon_{ij}^e$  ,  ${}^t \varepsilon_{ij}^p$  ,  ${}^t \varepsilon_{ij}^{th}$  ,  ${}^t \varepsilon_{ij}^{e'}$  가  
 $C^E$  ,  $\Lambda$   $\tau'$  deviatoric stress .  
 가

$$\int_v \sigma_{ij} \delta \varepsilon_{ij} dV = \int_v f_i^b \delta U_i dV + \int_s f_i^s \delta U_i dS \quad (15)$$

$$f_i^b , f_i^s , \delta U_i \quad S \quad (4).$$

sequential weak coupling analysis

PLANE 13

ANSYS Code

Birth and Death Option

가

가

Table 2

Table 3

7

8

4

lumped pass

가

bilinear

kinematic hardening

4.3

(1)

mesh

가

7

4

가

가

가

가

가

(5).

(2)

$s_z$

$s_x$

(4inch schedule 80)

(t/d)

0.075

x

Fig. 6

303MPa

가

HAZ

Fig. 7

Fig. 8

451MPa

가

HAZ

(6).

(3)

가 (t/d) 0.034 가 (10 inch schedule 40) Fig. 9 Fig. 10 Fig. 11 가 가 (7).

5.

316L (t/d=0.075) (t/d=0.034) 18 가 overmatch 가 가 Fig. 12 Fig. 13 가 450MPa Fig. 14 Fig. 15 가 306MPa 210MPa 가 가 (8).

1. , “ ”, KAERI/AR -508/98, pp 15~20, 1998.
2. H. Murakawa ,“Theoretical prediction of residual stress in welded structures, Welding International”, Vol.11, pp 2-7, 1997.
3. Man-jin Park, Dong-young Jang and Hee-dong Choi, “Residual stress measurement on welded specimen by neutron diffraction”, Journal of KWS, Vol. 20, April, 2002.
4. Newman, S., Z., “FEM model of 3D transient temperature and stress fields in welded plates”, ph. D. dissertation, Pittsburg, Pa., Carnegie-Mellon university, 1986.

5. J. B. Roelens, F. Maltrud and J. Lu, "Determination of residual stresses in submerged arc multi-pass welds by means of numerical simulation and comparison with experimental measurements", *Welding in the world*, Vol.33, pp36-43, 1994.

6. , , " ", *Journal of KNS*, October, 2002.

7. Tso-Liang Teng and Peng-Hsiang Chang, "A study of residual stresses in multi-pass girth-butt welded pipes", *International Journal of Pressure Vessels and Piping*, Vol.74, pp 59-70, 1997.

8. B. Brickstad, B. L. Josefson , "A parametric study of residual stress in multi-pass butt-welded stainless steel pipes", *International Journal of Pressure Vessels and Piping*, Vol.75, pp 11-25, 1998.

Table 1 Pipe and Weld Geometries

Standard	Pipe Weld	D (mm)	t (mm)	No. of Weld Pass
ANSI 4 inch Schedule 80	SMAW	114	8.56	7
ANSI 10 inch Schedule 40	SMAW	273	9.27	8

D= outside diameter, t= nominal pipe thickness

Table 2 Thermal Properties of Stainless Steel 316 L

T(°C)	C <sub>p</sub> (J/kg °C)	k(W/m °C)
40	450	15
400	570	20
800	620	25
1200	700	31
1390	730	33
1600	730	90

C<sub>p</sub>= Specific Heat, k= Thermal Conductivity

Table 3 Mechanical Properties of 316 L Stainless Steel and Weld Metal

T (°C)	E (GPa)	s <sub>y</sub> (MPa) Base	s <sub>y</sub> (MPa) Weld	E <sub>T</sub> (MPa)	ν	α (1/°C)
40	210	230	460	2800	0.26	19x10 <sup>-6</sup>
400	168	139	278	2370	0.32	19x10 <sup>-6</sup>
800	133	80	160	1900	0.25	19x10 <sup>-6</sup>
1200	55	22	22	600	0.24	19x10 <sup>-6</sup>
1390	10	2	2	100	0.24	19x10 <sup>-6</sup>
1600	10	2	2	100	0.24	19x10 <sup>-6</sup>

E= Elastic Modulus, s<sub>y</sub>= Yield Stress, E<sub>T</sub>=Tangent modulus, ν = Poission's Ratio, α = Linear Thermal Expansion Coefficient



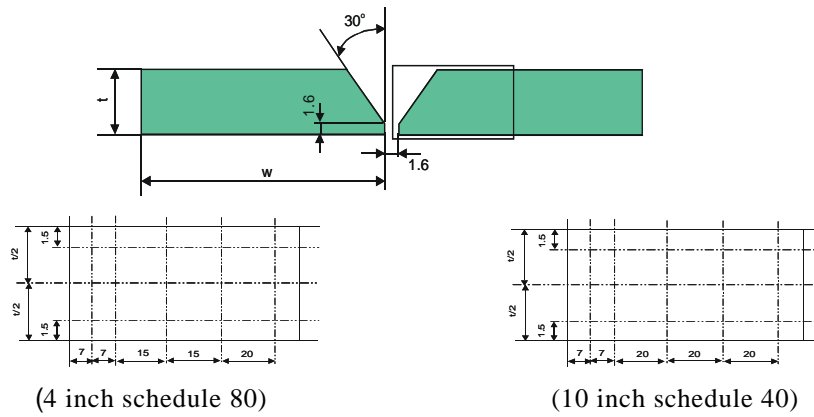


Fig. 1 Configuration of the weld joints and measurement points of the experiment

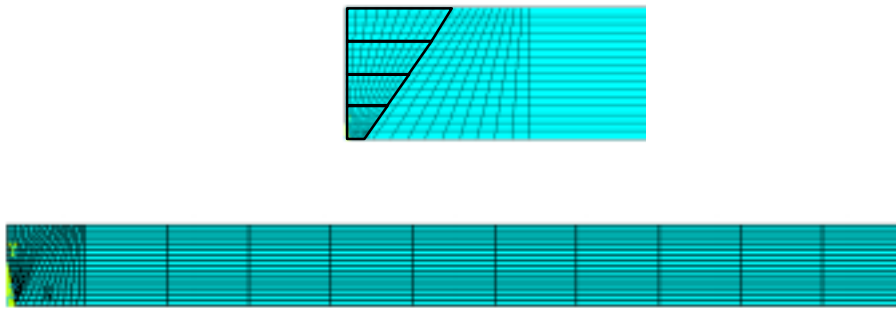


Fig. 2 Finite element model of analysis area

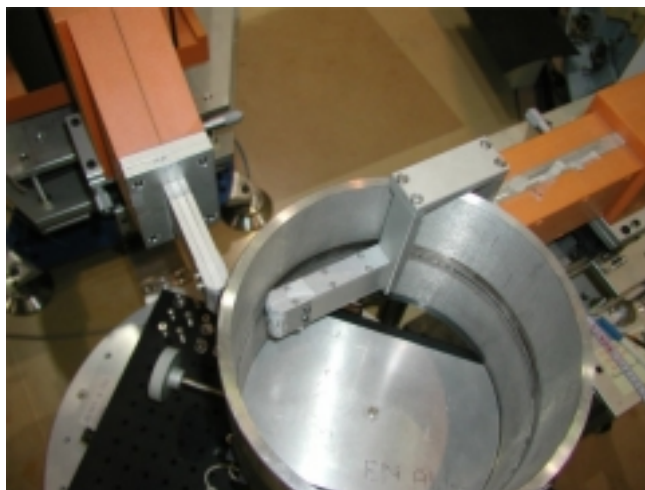


Fig. 3 Configuration of Large pipe specimen fixed in the sample stage

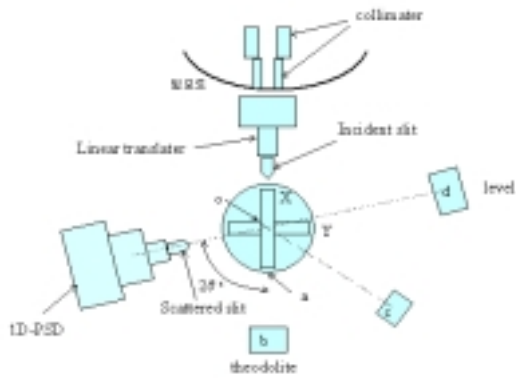


Fig. 4 Schematic diagram of experimental apparatus

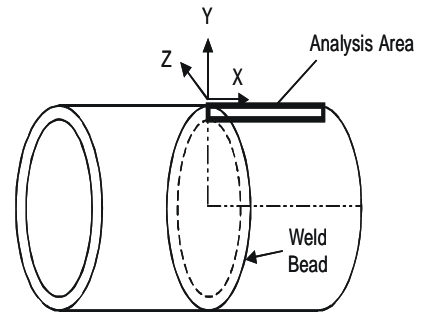


Fig. 5 Schematic diagram of multipass weld pipe

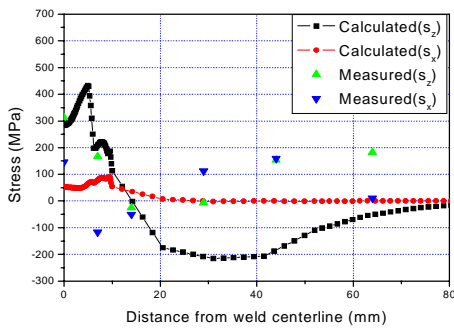


Fig. 6 Hoop and axial residual stress on outer surface(4 inch dia.)

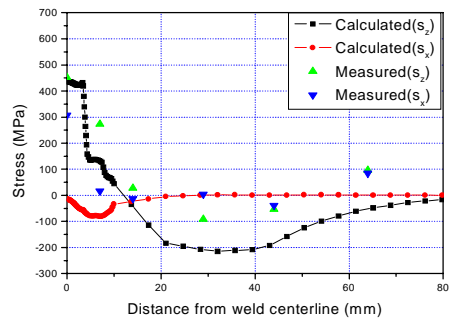


Fig. 7 Hoop and axial residual stress on middle surface (4 inch dia.)

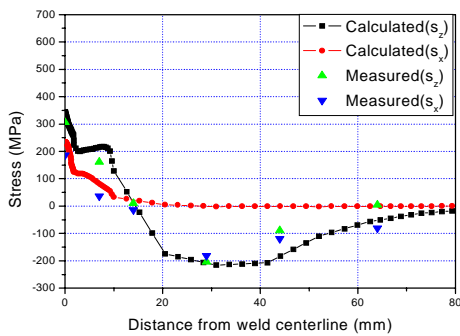


Fig. 8 Hoop and axial residual stress on inner surface(4 inch dia.)

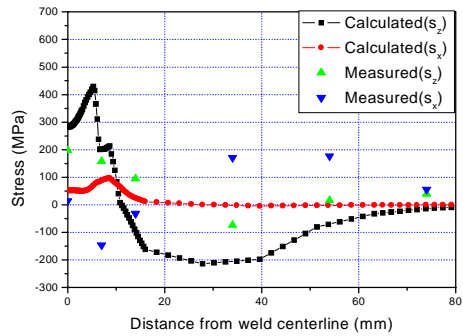


Fig. 9 Hoop and axial residual stress on outer surface(10 inch dia.)

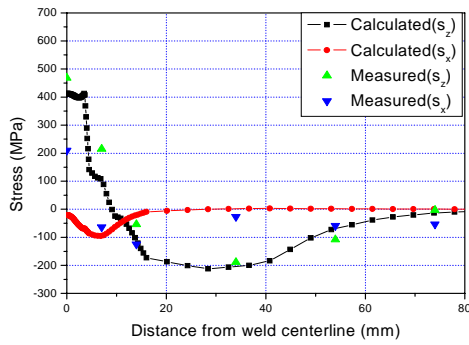


Fig.10 Hoop and axial residual stress on middle surface(10 inch dia.)

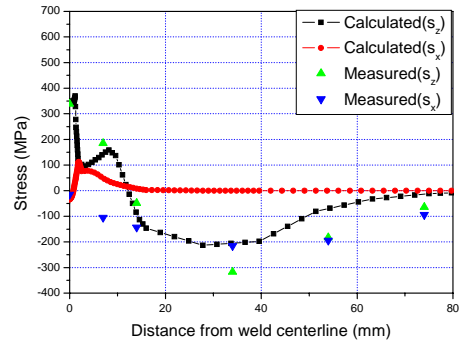


Fig. 11 Hoop and axial residual stress on inner surface(10 inch dia.)

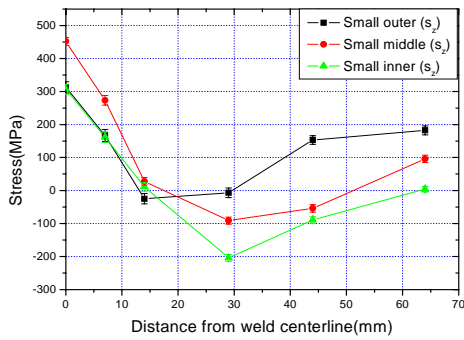


Fig. 12 Distribution of the hoop residual stress on the experimental data(Small pipe)

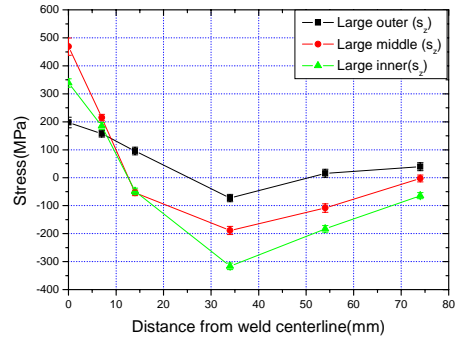


Fig. 13 Distribution of the hoop residual stress on the experimental data(Large pipe)

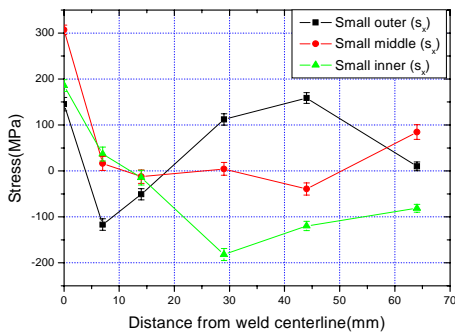


Fig. 14 Distribution of the axial residual stress on the experimental data(Small pipe)

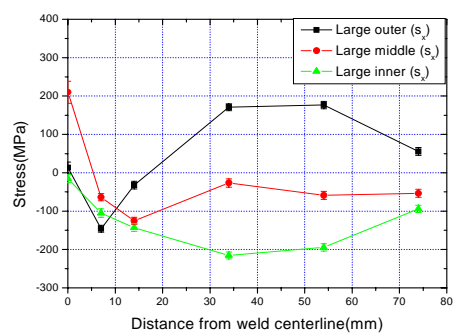


Fig. 15 Distribution of the axial residual stress on the experiment data(Large pipe)